It should be noted that B' would be constant at constant temperature.

The number of molecules striking per unit area per unit time is related to pressure P when the Maxwell-Boltzmann distribution law is used. In the actual rocket conditions, where the situation is far removed from equilibrium, this would be related to P^n, where n is any index $(1<n>0)$, so that for such a case

$$C_{\mathrm{Ads}}=C_m B' P^n/(1+B'P^n) \tag{7}$$

Since C_B^s has a fixed value, we have, from Eq. (3)

$$r=k'B'P^n/(1+B'P^n) \tag{8}$$

where k' is a constant and is given by

$$k'=kC_B^s C_m \tag{9}$$

Hence,

$$\dot{r}=r/\varphi=\frac{K'}{\varphi}\left[\frac{B'P^n}{1+B'P^n}\right]=\frac{k''B'P^n}{1+B'P^n} \tag{10}$$

Equation (10) predicts that, at very high pressure, when a complete monolayer has been formed,

$$\dot{r}=k'', \text{ since } B'P^n>>1 \tag{11}$$

In other words, the burning rate would tend towards a limit, as has been observed experimetally by Bernard et al.[4] Further, when $B'P^n<1$, one would have

$$\dot{r}=k''B'P^n \tag{12}$$

It is important to note that Eq. (10) agrees with the experimental results. The experimental, results of Bernard et al.[4] in the pressure range of 1-15 bars for nitric acid-urea systems are fitted by the following equation:

$$\dot{r}=0.25P^{0.88}/(1+0.37P^{0.80}) \tag{13}$$

The preceding ideas can be applied to the case of polymeric fuels also. The combustion process can be visualized as follows:

$$\text{Polymeric Fuel} + \text{Oxidizer} \rightarrow \begin{matrix}\text{Intermediate}\\ \text{Oxidative}\\ \text{Product}\end{matrix} \xrightarrow[\text{and Diffusion}]{\text{Decomposition}}$$

IV. Regression Rate of Solid Propellants

The foregoing arguments can be extended to the case of combustion of composite solid propellants also. The regression rate may be supposed to be made up of homogeneous reactions in the gas phase and heterogeneous, chemical reactions. We may therefore write,

$$\dot{r}=\dot{r}_{\mathrm{homo}}+\dot{r}_{\mathrm{hetero}}=\text{Constant}+\frac{k''B'P^n}{1+B'P^n} \tag{14}$$

where $\dot{r}_{\mathrm{homo}}$ is independent of pressure.

When $1>B'P^n$, we have,

$$\dot{r}=\text{constant}+a_1P^n \tag{15}$$

and further, when $a_1P^n>$ constant,

$$\dot{r}=a_1P^n \tag{16}$$

Equation (16) is preferred for actual application[11,12] when the chamber pressure does not exceed 2000 psia. In the intermediate situations, $\dot{r}$ would have complex dependence on pressure.

References

[1] Smoot, L.D. and Price, C.F., "Regression Rate of Nomentallized Hybrid Fuel Systems," *AIAA Journal*, Vol. 3, Aug. 1965, pp. 1408-1413.

[2] Smoot, L.D. and Price, C.F., "Regression Rates of Metallized Hybrid Fuel Systems," *AIAA Journal*, Vol. 4, May, 1966, pp. 910-915.

[3] Smoot, L.D. and Price, C.F., "Pressure Dependence of Hybrid Fuel Regression Rates," *AIAA Journal*, Vol. 5, Jan. 1967, pp. 102-106.

[4] Bernard, M.M., Michel, L., and Joulain, P., "Pressure Dependence of Liquid-Solid Ablation Rate," *Combustion Science and Technology*, Vol. 1, No. 6, 1970, pp. 471-480.

[5] Summerfield, M., Sutherland, G.S., Webb, M.J., Taback, H.J., and Hall, K.P., "Burning Mechanism of Ammonium Perchlorate Propellants," *Solid Propellant Rocket Research*, Edited by M. Summerfield, Academic Press, New York, 1960, pp. 141-182.

[6] Rastogi, R.P. and Singh, G., "Combustion of Composite Solid Propellants," *Journal of Scientific and Industrial Research*, 1975, (in press).

[7] Rastogi, R.P. and Kishore, K., "Polymers as Fuel Binders in Composite Solid Propellants," *Journal of Scientific and Industrial Research*, Vol. 32, June 1973, pp. 279-299.

[8] Spalding, D.B., *ARS Journal*, Vol. 29, 1959, pp. 828-835.

[9] Brzustowski, T.A., "Chemical and Physical Limits on Vapor-Phase Diffusion Flames of Droplets," *Canadian Journal of Chemical Engineering*, Vol. 43, 1965, pp. 30-35.

[10] Rastogi, R.P. and Munjal, N.L., "Mechanism and Kinetics of Pre-Ignition Reactions: Part I – Aniline-Red Fuming Nitric Acid Propellants," *Indian Journal of Chemistry*, Vol. 4, Nov. 1966, pp. 463-468.

[11] Loh, W.H.T., *Jet, Rocket, Nuclear, Ion and Electric Propulsion: Theory and Design*, Springer-Verlag, New York, 1968, p. 314.

[12] Barrere, M., Jaumotte, A., Fraeijs De Venbeke, B., and Vandenkerckhove, J. *Rocket Propulsion*, Elsevier Publishing Co., New York, 1960, p. 195.

Unsteady Local Linearization Solution for Pulsating Bodies at $M_\infty = 1$

Stephen S. Stahara*
Nielsen Engineering & Research, Inc., Mountain View, Calif.
and
John R. Spreiter†
Stanford University, Stanford, Calif.

Introduction

With the continuing development of successful techniques for solving steady transonic flows, considerable interest has been focused recently on the development of methods to solve unsteady transonic problems.[1] In this note we describe the local linearization solution for transonic flow past slender bodies of revolution undergoing oscillatory pulsatile motion of the body surface. This result provides the fundamental unsteady source solution from which higher-order multipole solutions (dipole, etc.) necessary to describe more complex unsteady motions (e.g., translation, rotation) can be obtained. The theory is based on the concept of dividing the flow into steady and unsteady

Received December 4, 1975; revision received April 5, 1976. This work was supported by the Office of Naval Research under Contract No. N00014-73-C-0379.

Index categories: Nonsteady Aerodynamics, Subsonic and Transonic Flow.

*Senior Research Scientist. Member AIAA.

†Professor, Department of Aeronautics and Astronautics and Mechanical Engineering; also consultant to Nielsen Engineering & Research, Inc. Fellow AIAA.

components and solving the resultant equations by the local linearization method.[2] The analysis is developed generally for sonic and near sonic flows, with specific applications made to parabolic-arc half-bodies and cones at freestream Mach number $M_\infty = 1$. The results indicate the correct convergence to nonlinear quasisteady theory as the reduced frequency of oscillation based on body length, $k \to 0$, and to linear acoustic theory as k becomes large ($k \geq 1$). For $k \leq 1$, a range of prime importance in many flutter and stability applications, the unsteady solutions exhibit a significant nonlinear thickness effect induced by the steady-state solution, much like that displayed in the two-dimensional case.[3] This indicates a basic shortcoming of linear theory in this frequency range.

Analysis

The concept that a major body of transonic flow problems can be predicted accurately within the framework of inviscid, nonlinear small-disturbance theory, described by the equation

$$(1-M_\infty^2)\phi_{xx}+\phi_{rr}+\frac{1}{r}\phi_r+\frac{1}{r^2}\phi_{\theta\theta} = M_\infty^2(\gamma+1)\phi_x\phi_{xx}+M_\infty^2\phi_{tt}+2M_\infty^2\phi_{xt} \quad (1)$$

has been well-established.[4,5] In Equation (1), M_∞ is the freestream Mach number; (x,r,θ) are nondimensional body-fixed cylindrical coordinates with (x,r) normalized by body length ℓ and with the x-axis directed rearward and aligned with the body centerline; t is nondimensional time normalized by ℓ/U_∞, where U_∞ is the freestream velocity; γ is the ratio of specific heats equal to 7/5 for air; and ϕ is the dimensionless perturbation velocity potential. Although a variety of subcases of Eq. (1) exist[4,6] depending upon whether the time behavior of the motion is very slow (quasisteady: ϕ_{xt}, ϕ_{tt} neglected), somewhat more rapid (mildly uinsteady: ϕ_{tt} neglected), or very rapid (linear high frequency: $\phi_x\phi_{xx}$, ϕ_{xt} neglected, the authors have considered the more general case, encompassing all frequencies given by Eq. (1).

For the general axisymmetric oscillatory flows considered here, it is convenient to expand the solution into a steady and unsteady component. Thus, set

$$\phi(x,r,\theta,t) = \phi_I(x,r) + \text{R.P.}[\tilde{\phi}(x,r)e^{ikt}] \quad (2)$$

where ϕ_I is the axisymmetric steady perturbation potential, which satisfies Eq. (1) with the θ and t terms omitted, $\tilde{\phi}$ is the complex amplitude of the oscillatory perturbation velocity potential, k is the reduced frequency defined by $k=\omega\ell/U_\infty$, and R.P. signifies the real part of a complex quantity. Based on the assumption that small-amplitude oscillations are appropriate for flutter and stability analysis, the equation for $\tilde{\phi}$ becomes

$$\tilde{\phi}_{rr}+(1/r)\tilde{\phi}_r = [M_\infty^2 - 1 + M_\infty^2(\gamma+1)\phi_{Ix}]\tilde{\phi}_{xx} + [M_\infty^2(\gamma+1)\phi_{Ixx}+2iM_\infty^2 k]\,\tilde{\phi}_x - M_\infty^2 \rho^{\cup}\tilde{\phi} \quad (3)$$

which, although linear, nevertheless, remains formidable because of the variable coefficients and mixed elliptic-hyperbolic type.

The boundary condition at the body surface can be decomposed analogously. Upon setting

$$R(x,t) = \epsilon\bar{R}(x) + \text{R.P.}[\delta\tilde{R}(x)e^{ikt}] \quad (4)$$

where $(\bar{R}, \tilde{R})$ are normalized functions describing the steady and oscillatory components of the body ordinates, and (ϵ,δ) are, respectively, the normalized maximum body thickness and the dimensionless amplitude of the unsteady oscillations, one obtains

$$\phi_{Ir}(x,R_I) = R_I' + O(\epsilon^3 \ell\,\mathrm{n}\epsilon) \quad (5a)$$

$$\tilde{\phi}_r(x,R_I) = \delta\left[\tilde{R}' + ik\tilde{R} + \frac{\bar{R}'}{\bar{R}}\tilde{R}\right] + O(\delta\epsilon^2 \ell\,\mathrm{n}\epsilon\delta^2) \quad (5b)$$

where $R_I = \epsilon\bar{R}$, and primes indicate differentiation with respect to x. The first two terms on the right-hand side of Eq. (5b) are familiar, since they also appear in the oscillatory thin-wing problem.[5] For the slender body case, however, the third term arises from the imposition of the no-flow boundary condition at the actual oscillating body surface,[7] where a Taylor series expansion about the mean position $r=R_I$ is used to remove the resulting implicit dependence on δ. Finally, the corresponding expressions for the surface pressure coefficients are

$$C_{p_I}(x,R_I) = -2\phi_{Ix}(x,R_I) - R_I'^2 \quad (6a)$$

$$\tilde{C}_p(x,R_I) = -2\left[\tilde{\phi}_x(x,R_I) + ik\tilde{\phi}(x,R_I) + \left(R_I'' + \frac{R_I'^2}{R_I}\right)\tilde{R} + R_I'(\tilde{R}' + ik\tilde{R})\right] \quad (6b)$$

Use of the method of matched asymptotic expansions serves to identify the logarithmic behavior of both the steady and unsteady components near the body axis. Consequently, the differential equation and surface boundary condition for the unsteady component can be expressed in the compact form

$$\lambda_I\tilde{\phi}_{xx} + \lambda_2\tilde{\phi}_x + \lambda_3\tilde{\phi} = \tilde{\phi}_{rr} + (1/r)\tilde{\phi}_r \quad (7)$$

$$\lim_{r\to 0}(r\tilde{\phi}_r) = g(x) = \epsilon\delta\bar{R}[\tilde{R}' + ik\tilde{R} + (\bar{R}'/\bar{R})\tilde{R}] \quad (8)$$

where $(\lambda_I, \lambda_2, \lambda_3)$ can be identified from Eq. (3).

Three fundamentally different differential equations and solutions occur for $\tilde{\phi}$, depending upon the sign of λ_I; i.e., whether $\lambda_I < 0$ (subsonic), $\lambda_I = 0$, (sonic), or $\lambda_I > 0$ (supersonic). The regions are illustrated in the upper left of Fig. 1 for the forepart of a slender convex body at $M_\infty = 1$. The solution for the sonic region 2 must merge continuously with that for the subsonic region 1 ahead of it and the supersonic region 3 behind it.

The procedure for determining the local linearization solution for the unsteady component $\tilde{\phi}$ requires first that the steady-state solution ϕ_I be obtained to evaluate the variable coefficients (λ_I, λ_2). Then an approximate solution for $\tilde{\phi}$ is determined by replacing the variable coefficients (λ_I, λ_2) temporarily in Eq. (7) by constants, and solving the simplified equations that result in each of the three regions identified previously. In the original procedure for steady transonic flow, the next step would be to calculate the surface acceleration $d^2\tilde{\phi}(x,R_I)/dx^2$, replace the constants (λ_I, λ_2) by

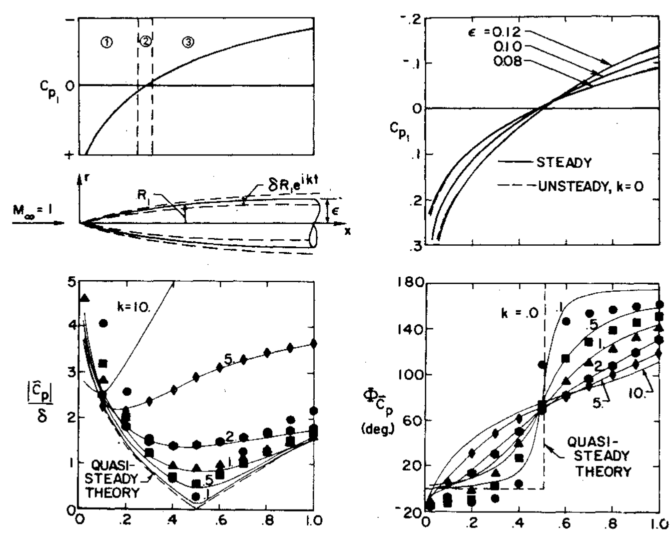

Fig. 1 Unsteady pressure distributions on various parabolic-arc half-bodies undergoing pulsatile surface oscillations; local linearization ——, quasi steady ---, acoustic theory $k=0.01$, ●; $k=0.5$, ■; $k=1.0$, ▲; $k=2.0$, ⬢; $k=5.0$ ◆.

the functions that they original represented, and finally integrate the resultant second-order ordinary differential equation along the body surface to obtain both $d\tilde{\phi}(x,R_l)/dx$ and $\tilde{\phi}(x,R_l)$, to be used in Eq. (6b). In the results reported here, the authors have used a variant of that procedure by calculating $\tilde{\phi}_x(x,R_l)$ and $\tilde{\phi}(x,R_l)$ directly from the simplified equations. Near the body surface, these solutions are

$$\tilde{\phi}(x,r)_{\text{sonic}} = \frac{1}{2}\left[g(x)\cdot\left\{E_{\text{in}}(A_0x)+\ell n\left(\frac{\lambda_2 r^2}{4x}\right)+C\right\} + \int_0^x \frac{g(x)-g(\xi)}{x-\xi}e^{-A_0(x-\xi)}d\xi\right] \qquad (\lambda_1 \simeq 0) \qquad (9)$$

$$\tilde{\phi}(x,r)_{\text{subsonic}} = \frac{1}{2}\left[g(x)\cdot\left\{E_{\text{in}}(A_lx)+E_{\text{in}}[-A_2(1-x)] + \ell n\left(\frac{-\lambda_l r^2}{4x(1-x)}\right)\right\} + \int_0^x \frac{g(x)-g(\xi)}{x-\xi}e^{-A_l(x-\xi)}d\xi - \int_x^l \frac{g(\xi)-g(x)}{\xi-x}e^{A_2(\xi-x)}d\xi\right] \qquad (\lambda_l<0) \qquad (10)$$

$$\tilde{\phi}(x,r)_{\text{supersonic}} = \frac{1}{2}\left[g(x)\cdot\left\{E_{\text{in}}(A_lx)+E_{\text{in}}(A_2x)+\ell n\left(\frac{\lambda_l r^2}{4x^2}\right)\right\} + \int_0^x \frac{g(x)-g(\xi)}{x-\xi}\left\{e^{-A_l(x-\xi)}+e^{-A_2(x-\xi)}\right\}d\xi\right] \qquad (\lambda_l>0) \qquad (11)$$

where $E_{\text{in}}(Z)$ is the complete exponential function of complex argument Z,[8] C is Euler's constant,

$$A_0=\lambda_3/\lambda_2, \quad A_l=[\lambda_2-(\lambda_2^2-4\lambda_l\lambda_3)^{1/2}]/2\lambda_l$$

and

$$A_2=[\lambda_2+(\lambda_2^2-4\lambda_l\lambda_3)^{1/2}]/2\lambda_l$$

Results determined by employing the solutions given by Eqs. (9-11) in their respective domains, are shown in Fig. 1. Exhibited in the two lower plots are the normalized magnitude and phase (in degrees) of the unsteady surface pressure distributions $\tilde{C}_p$ for a parabolic-arc half-body, with $\epsilon=0.10$ executing pulsatile oscillations of its body surface proportional to the local radius ($\tilde{R}=\bar{R}$). In those results, as well as others presented here, the steady solutions required as input to the unsteady calculation were determined by the local linearization method for axisymmetric bodies,[2] which is known to provide good accuracy for the shapes being considered. Also indicated on those plots are the results provided by quasisteady theory and by linear acoustic theory, to which the present results converge for small and large k. The close correspondence between the nonlinear and quasisteady results for $k=0.1$ implies a substantial nonlinear thickness effect of the steady flow upon the unsteady component at low frequencies, and indicates, furthermore, the quasisteady theory can provide good results in this range. In contrast, the comparisons with acoustic theory indicate large discrepancies for small k, particularly in phase angle, which tend to disappear only when k is approximately 2.

A further evaluation of the low-frequency results predicted by the present method is provided by the plot in the upper right of Fig. 1. The pressure distributions indicated by the unsteady analysis for a basic parabolic-arc half-body, having a maximum thickness $\epsilon=0.10$, undergoing slow expansion to $\epsilon=0.12$ and contraction to $\epsilon=0.08$, are compared with results predicted by the local linearization theory for steady flow past

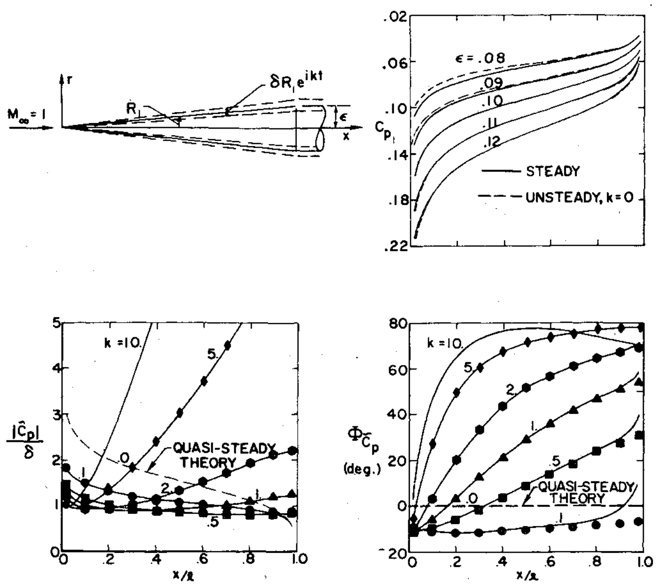

Fig. 2 Unsteady pressure distributions on various cones undergoing pulsatile surface oscillations; local linearization ——, quasi-steady – – –, acoustic theory $k=0.1$, ●; $k=0.5$, ■; $k=1.0$, ▲; $k=2.0$, ⬣; $k=5.0$, ◆.

three such bodies. The results are in good agreement, in spite of the linearization of the unsteady component and the substantially different methods of solution.

Figure 2 shows the analogous results for a cone with $\epsilon=0.10$. Although the analysis derived here applies strictly to smoothly accelerating flows on continuous bodies – a condition severely strained for the flow in the vicinity of the shoulder on a cone – application of the previous techniques is still possible by adopting the strategy of using the unsteady sonic solution predicted by the current method along the entire length of cone. This is plausible, since the subsonic solution, which normally would be joined to the sonic result for points in the region ahead of the shoulder, in fact becomes ill-conditioned; this is because, for a cone, the sonic point is fixed at the end of the body. Again, the quasisteady predictions of the present method shown in the upper right-hand plot of Fig. 2 indicate very good agreement with the steady state results, whereas the comparisons with the acoustic theory results shown in the bottom plots indicate a much more rapid approach to acoustic theory as the frequency increases for a cone, in contrast to a parabolic-arc half body.

References

[1]Spreiter, J.R. and Stahara, S.S., "Unsteady Transonic Aerodynamics – An Aeronautics Challenge," in *Unsteady Aerodynamics, Proceedings of a Symposium held at University of Arizona, March 18-20, 1975*, edited by R. B. Kinney, Vol. II, July 1975, pp. 553-581.

[2]Speiter, J. R. and Alksne, A. Y., "Slender Body Theory Based on Approximate Solution of the Transonic Flow Equation," NASA TR R-2, 1959.

[3]Spreiter, J. R. and Stahara, S.S., "Nonlinear Unsteady Transonic Flow Theory – Local Linearization Solution for Two-Dimensional Flow," *AIAA Journal*, Vol. 13, June 1975, pp. 719-720.

[4]Miles, J. W., *The Potential Theory of Unsteady Supersonic Flow*, Cambridge University Press, New York, 1959.

[5]Landahl, M.T., *Unsteady Transonic Flow*, Pergammon Press, London, 1961.

[6]Landahl, M.T., "Linearized Theory for Unsteady Transonic Flow," in *Symposium Transsonicum*, edited by K. Oswatitisch, Springer-Verlag, Berlin/Gottingen/Heidelberg, 1964, pp. 414-439.

[7]Hoffman, G. H. and Platzer, M. F., "On Supersonic Flow Past Oscillating Bodies of Revolution," *AIAA Journal*, Vol. 4, Feb. 1966, pp. 370-371.

[8]Abramowitz, M. and Stegun, I. A., *Handbook of Mathematical Functions*, National Bureau of Standards, Washington D.C., Aug. 1966, Fifth Printing, p. 228.